

**SHAPE MEASUREMENT SIMULATION FOR THE SILICON TRENCH**  
**BY SCATTERING PROPERTIES AND CONTINUOUS WAVELET ANALYSIS**  
**WITH INTERFERENCE SPECTROSCOPY**

Hirokimi Shirasaki

Tamagawa University, Electrical Engineering Dept., 6-1-1 Tamagawa-Gakuen, Machida, Tokyo 194-8610, Japan

E-mail: [shira@eng.tamagawa.ac.jp](mailto:shira@eng.tamagawa.ac.jp)

**ABSTRACT**

The scattering properties made by the irradiated two dimensional Gaussian beams in the square trench are analyzed by the boundary element method and the FDTD method. We investigate the scattering patterns by changing the depth and the width of the trenches, and the polarization and the incidence angles of the beams. Then, we calculate the interference spectrum data by using the wavelength dispersion because the silicon substrate is thought to be a dispersive and the dielectric has energy loss in the visible light range. The trench depths are examined by the continuous wavelet analysis with the interference spectrum data.

**INTRODUCTION**

In a depth measurement of trench holes [1] on a semiconductor substrate by interference spectroscopy, we sometimes cannot measure the depth when a diameter approaches a visible light wavelength. To investigate the cause, we determined the delay properties from the reflected intensity data obtained by the interference spectroscopy [2]. Then, we confirmed that the delay time in the short wavelength is nearly equal to the time taken by the light to reach the bottom and return to the entrance. However, we found that when the trench diameter approaches the wavelength used in the measurements, the delay change becomes longated.

In this paper, we investigate whether the trench figures of widths under the cutoff wavelengths are investigated by the light scattering properties. The scattering properties made by the irradiated two dimensional Gaussian beams in the square trench are analyzed by the boundary element method (BEM) [3] and the finite-difference time-domain (FDTD) method. Then, we investigate the scattering patterns by changing the depth, the width and the pitch of the periodic trench, the polarization and the incidence angle of the beams. Then, the trench depth is examined by the continuous wavelet analysis with the interference spectrum data [4].

**ANALYSIS**

**Two dimensional Gaussian beam**

The coordinates system is shown in Fig.1. The E polarized electric fields (E) and the H polarized magnetic fields (H) only have z direction components with no other components considered. The incidence 2D Gaussian beams are given by;

$$u^{in} = \begin{pmatrix} E_0 \\ H_0 \end{pmatrix} \Phi(x', y'), \quad (1)$$

where

$$\Phi(x', y') = \sqrt{\frac{\omega_0}{\omega(y')}} \cdot \exp \left\{ -j(ky' - \Psi(y')) - (j \frac{2y'}{k\omega_0} + 1) \frac{x'^2}{\omega(y')} \right\} \quad (2)$$

$$\omega^2(y') = \omega_0^2 \left\{ 1 + \left( \frac{2y'}{k\omega_0^2} \right)^2 \right\}, \quad (3)$$

$$\Psi(y') = \frac{1}{2} \tan^{-1} \left( \frac{2y'}{k\omega_0^2} \right) \quad (4)$$

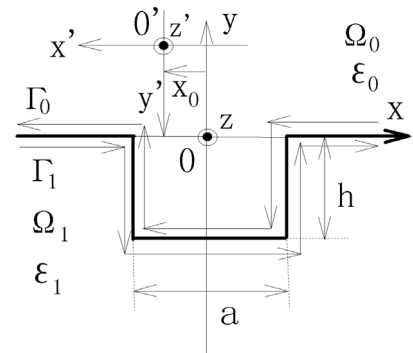


Fig.1 Analytical model.

and the  $k$  is a wavenumber, and the  $\omega_0$  are beam waists. We call the E polarized light, the TM mode and the H polarized light, the TE mode according to the definition of FDTD analysis.

### Boundary element method

The BEM of the 2D Helmholtz equation is analyzed by using a constant element [5]. Scattered waves ( $u$ ) satisfy the Helmholtz equation. By adding known electric fields and magnetic fields into the boundary, it is possible to obtain unknown electric fields and magnetic fields in a specific place. In this method, the losses of substrates cannot be included. In Fig.1, the area  $\Omega_0$  is a semi-infinite free space (the permittivity is  $\epsilon_0$ ). The area  $\Omega_1$  is a dielectric space. In this case, we apply the BEM technique as they are independent in each partial area. The analysis for obtaining the scattering characteristic of light from the dielectric trench using the BEM s described in Ref. [3].

### FDTD Analysis

The FDTD method is to approximate the Maxwell equation by a finite difference and to solve by the time domain [6]. The analytic region includes a source and scattering fields and is divided by small cells. The losses of substrates can be included by the FDTD method. Because this method is for a closed region problem, the perfectly matching layer (PML) is used as absorbing conditions for an open region problem. In this paper, we simulate the incidence 2D Gaussian beams interacting with the silicon groove substrate. The far fields are obtained by integrating equivalent electric and magnetic currents on a closed contour generated in the near fields [7].

### WIDTH MEASUREMENT

#### Width measurements using the FDTD method

We define the periodic groove surface width,  $a$ , the bottom widths,  $b$  and the pitch,  $a+b$ . Figure 2 shows the distribution of electric fields  $E_z$  interacting with the silicon periodic grooves using a width of  $a=0.1(\mu\text{m})$  and a depth of  $h=0.2(\mu\text{m})$ . The cell size for FDTD analysis is  $\Delta x=\Delta y=0.01(\mu\text{m})$ . The trench surface is located larger than  $x=40\Delta x$ . The beam waist is  $\omega_0=2(\mu\text{m})$  and the wavelength is  $\lambda=0.6328(\mu\text{m})$ . The substrate extinction coefficients are included. The beam is irradiated from an incident angle of  $\theta_{\text{in}}=100(\text{deg.})$  which is measured from the trench surface (x-axis).

The far fields are obtained by integrating equivalent electric and magnetic currents on a closed contour generated in the near fields[7]. Figure 3 shows the far fields for the periodic grooves. The Gaussian beams of TM and TE modes have the parameters of  $\omega_0=2(\mu\text{m})$ ,  $\lambda=0.6328(\mu\text{m})$  and  $\theta_{\text{in}}=100(\text{deg.})$ . The pitch is  $0.36(\mu\text{m})$ , and the widths,  $a$ , are changed from  $0.18$  to  $0.24(\mu\text{m})$ . As the peak levels at  $\theta_{\text{out}}=80(\text{deg.})$  change well, we can measure the width.

#### Width measurements using the BEM

The far field patterns for periodic groove are obtained using BEM. The scattering properties with a radius  $r=800(\mu\text{m})$  are examined from the originating point of which the shape of the waves almost become constant. Then, we obtain the amplitude and the phase properties of the reflection angle at  $\theta_{\text{out}}=80(\text{deg.})$  to investigate the narrower groove widths of  $a=b=0.07-0.2(\mu\text{m})$ . We use the same widths for

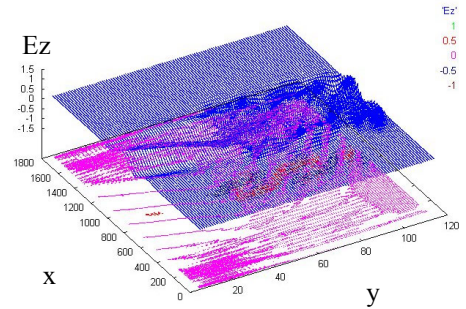
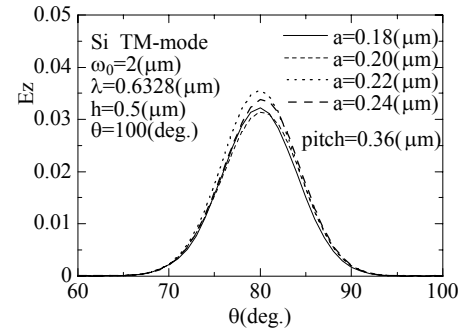
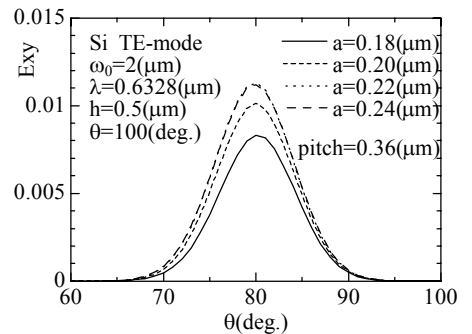


Fig.2 Propagation property. [ TM mode, Periodic groove, pitch= $0.36(\mu\text{m})$ ,  $a=0.18(\mu\text{m})$ ,  $h=0.5(\mu\text{m})$ ,  $\theta_{\text{in}}=100(\text{deg.})$ ]



(a) TM mode



(b) TE mode

Fig.3 Scattering properties of periodic grooves.

the periodic groove surface and bottom widths. Figure 4(a) shows the ratios of TE and TM mode amplitude (TE/TM). Figure 4(b) shows the differences between the TE and the TM mode phases (TE-TM). The amplitude differences do not show the regularity but the phase differences show the regularity. The TM mode phases are nearly constant for the fine grooves because the TM modes have cutoff properties but do not recognize the grooves. The TE mode phases change for the fine grooves because the TE modes do not have cutoffs but recognize the grooves. Therefore we can measure the narrow widths using the phase differences.

## DEPTH MEASUREMENT

### Interference spectral waveforms using BEM

The relative permittivities and the extinction coefficients of silicon substrates are changed by wavelength. Hereafter, we calculate the scattering properties using this wavelength dispersion. Figures 5 shows the frequency characteristics of the interference spectrum waveforms of TM and TE modes in the direction of y. The width is  $0.4(\mu\text{m})$ . The interference spectral diffraction waveform is within 400 to 780(THz). Every sampling frequency,  $f_s$ , is 1(THz). The cutoff occurs in the frequency of  $f=375(\text{THz})$  or less in the TM mode for the perfect conductor [8]. In Fig. 5(a), the interference does not occur in the dielectric trench in the vicinity of the cutoff frequency. There is no cutoff when the TE mode is used so it is understood to cause interference below the cutoff frequency in Fig. 8(b).

### Depth measurements using wavelet analysis

The continuous wavelet analysis for the interference spectrum waveform is made by the Daubechies wavelets (the order 2). In Fig. 6, the TM mode's wavelet analysis results for the waveform in Fig. 5(a) are shown in the contour diagrams. The width is  $0.4(\mu\text{m})$ . In the wavelet analysis, the horizontal axis does not change and the frequency is shown. The vertical axis is converted into scales and the signal strength is shown in the z axis. The scales is corresponding to the reciprocal of time. When the width is  $a=0.4(\mu\text{m})$ , the TM mode is intercepted under the frequency [ $f=375(\text{THz})$ ] and the light does not enter the trench. If the depth becomes deeper, the signals from the trench become smaller. Then, the signal components appear over  $f=500(\text{THz})$  at  $h=2(\mu\text{m})$  and  $f=550(\text{THz})$  at  $h=3(\mu\text{m})$ .

In Fig. 7, the TE mode does not have a cutoff. There are signal components (shown as a series of ovals) over the whole frequency. In Fig. 8, we show the relation between the depths and the reciprocals of scales peak values. The reciprocals of scales are proportional to the depths because the reciprocals of scales are corresponding to the times and the depth is obtained by the multiplication of time and light velocity. Each depth was not obtained continuously in the FFT processing [8] but it is continuous in the wavelet analysis. Then, the result in the wavelet analysis is more detailed than the FFT processing. In Fig. 8, we also show the reciprocals of scales for the taper trenches which are plotted on the positions corresponding to the cutoff depths. The tapers change the width along to the depth and the entrance widths are  $0.4(\mu\text{m})$  and the bottom widths are  $0.04(\mu\text{m})$ . The reciprocals of scales for the TE mode tapers are nearly equal to that of the rectangle groove depth [ $3(\mu\text{m})$ ] in Fig. 8(b). The TE modes do not have the cutoffs and the lights go through the bottoms. Because the TM modes have the cutoff properties, the lights are estimated to reflect on the way of tapers. In Fig. 8(a) when the depth is  $h=2(\mu\text{m})$  we can see the TM modes do not reach the bottom and do not reflect at the cutoff points instantly. When the lights go through the

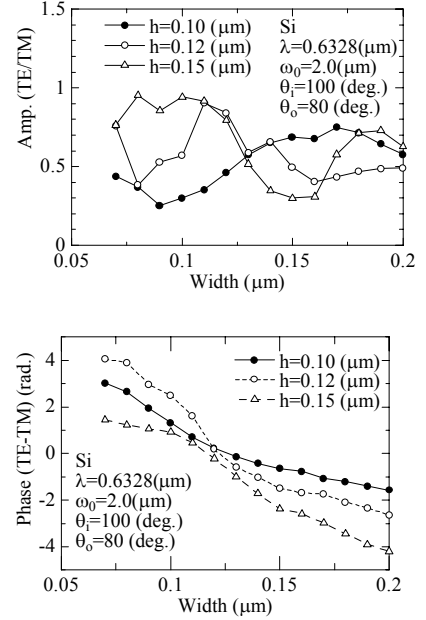


Fig.4 Relative amplitudes and phases.

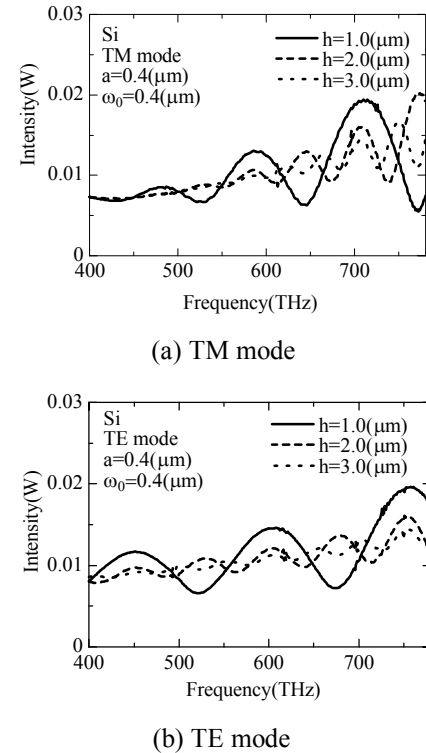


Fig.5 Interference spectral waveform.

cutoff width, the lights penetrate over the cutoff depths exponentially and the velocity delay dispersions occur.

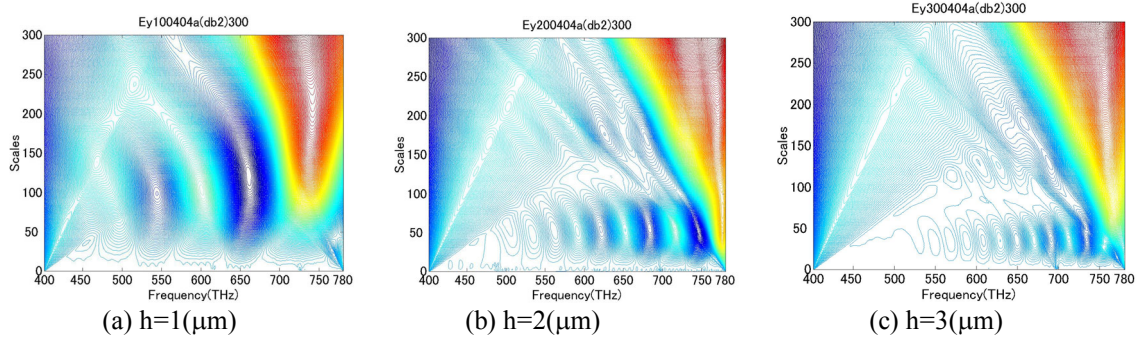


Fig.6 Wavelet analysis. [ TM mode, Single groove,  $a=0.4(\mu\text{m})$ ,  $\omega_0=0.4(\mu\text{m})$ ,  $\lambda=0.6328(\mu\text{m})$ ]

## CONCLUSION

The scattering properties made by the irradiated 2D Gaussian wave beams in the square trench were analyzed by the BEM and the FDTD method. Then, we investigated the scattering properties changes by changing the trench width. Then, the trench depth was examined by the continuous wavelet analysis with the interference spectrum data. The reciprocals of scales was proportional to the depths and the depth were obtained by the charts which showed the relationships between the reciprocals of scales and the depths. Finally, the tapered trenches were analyzed using the wavelet analysis. We will study more complicated shaped grooves in detail in months to come.

## ACKNOWLEDGEMENTS

The author wishes to thank for Mr. Noriyuki Kondou, Mr. Kunio Ueta, Dinippon Screen Mfg. Co.Ltd for their helpful comments and friendship, and my laboratory students for their helpful calculations.

## REFERENCES

- [1] K. Harafuji and N. Nomura: "On the image brightness of the trench bottom surface in a scanning electron microscope," J. Appl. Phys., Vol.72, pp.2541-2548, October 1992.
- [2] H. Shirasaki, N. Kondo and A. Abematsu: " Delay properties of optical wave in semiconductor trench for depth measurement using interference spectroscopy," Jpn. J. Appl. Phys., Vol. 32, pp. 3502-3506, August 1993.
- [3] H. Shirasaki, "Depth and width measurement simulation of semiconductor trench by optical wave irradiation," IEEE, Trans. Magnetics, Vol. 33, No. 2, pp. 1428-1431, March 1997.
- [4] H. Shirasaki, "The depth measurement simulation for the dielectric trench by continuous wavelet analysis with interference spectroscopy," ICSPAT '00, October 2000.
- [5] C.A.Brebbia, J.Dominguez: "Boundary elements: An introductory course, " McGraw-Hill, chap.2, 1989.
- [6]. A. Taflove and S.C. Hagness: "Computational electrodynamics: The finite-difference time-domain method, " Artech House, 2000.
- [7] K.S. Kunz and R.J. Luebbers: "The finite difference time domain method for electromagnetics," CRC Press, chap.7 1993.
- [8] H. Shirasaki, "Depth measurement simulation of dielectric trench by FFT processing of interference spectroscopy," ICSPAT '99, November 1999.

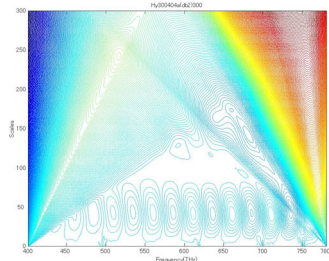
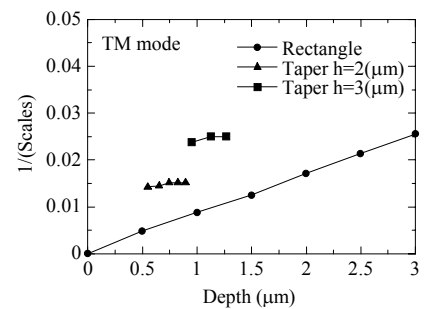
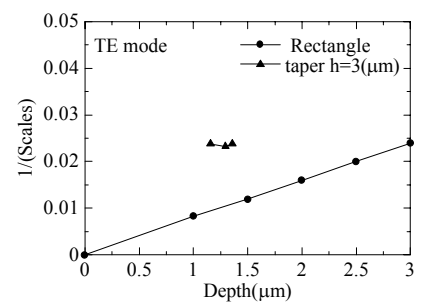


Fig.7 Wavelet analysis. [TE mode, Single groove,  $h=3(\mu\text{m})$ ,  $a=0.4(\mu\text{m})$ ,  $\omega_0=0.4(\mu\text{m})$ ]



(a) TM mode



(b) TE mode

Fig.8 Relationships between the depths and the reciprocal of scales. [Single groove,  $a=0.4(\mu\text{m})$ ,  $\omega_0=0.4(\mu\text{m})$ ]